ESTIMATING THE FUNDAMENTAL FREQUENCY OF A PROPELLER SHAFT–BLADE HARMONIC SERIES USING THE HILBERT TRANSFORM AND AUTOCORRELATION

O. V. Babikov* and V. G. Babikov**

*,**Trapeznikov Institute of Control Sciences, Russian Academy of Sciences, Moscow, Russia

*✉ babikov.ov@phystech.edu, **✉ babikov@ipu.ru

Abstract. The problem of estimating the fundamental frequency of a harmonic series arises in many areas of science and technology. For example, in vibration diagnosis, it is required to estimate the wear of bearings by the shift of the base of a harmonic series. In audio signal processing, this problem is associated with automatic instrument tuning. In speech synthesis, the fundamental frequency determines the pitch. In speech recognition, the frequency of the fundamental tone is an important information feature. In radio engineering, this problem is solved for the purpose of signal restoration, filtering, and decoding. In biomedical engineering, when analyzing a patient's ECG, EEG, voice, or breathing, pathologies such as arrhythmia are diagnosed by the fundamental frequency. In the detection and classification of sea vessels, the most significant information criterion is the base of a propeller shaft–blade harmonic series. This paper proposes new approaches to estimating the fundamental frequency in high noise conditions. To reduce errors, the idea is to use the method of periodograms, filtering, autocorrelation, and the Hilbert transform. Note that in high noise conditions, the estimate of the fundamental frequency of a harmonic series is significantly improved by selecting optimal parameters: the size of the time window, filtering parameters, the spectrum interval for autocorrelation, and the number of autocorrelations.

Keywords: fast Fourier transform, discrete Fourier transform, autocorrelation, Hilbert transform, fundamental frequency.

INTRODUCTION

When estimating the fundamental frequency, the original general problem is concretized considering particualr differences in the types of signals and noise and signal-noise mixture preprocessing methods. This paper addresses the problem of finding the base of a *propeller shaft–blade harmonic series* (PSBHS) generated by a sea vessel, although the methods proposed are also applicable in other engineering disciplines. Propellers are a main source of the primary hydroacoustic field of sea vessels. They generate vibrations at two key discrete frequencies: at the rotational frequency of the shaft (the shaft frequency) and the frequency representing the product of the shaft frequency and the number of propeller blades (the blade frequency) [1, 2]. For modern vessels, shaft frequencies commonly lie between 1 Hz and 6 Hz whereas blade frequencies between 6 Hz and 24 Hz [3].

Due to nonlinear effects during the emission of acoustic waves, a set of harmonics with multiple frequencies arises in the low-frequency spectrum of vessel noise. The amplitude of these harmonics, called discrete components, significantly exceeds the ambient noise level. A group of such discrete components located at multiple frequencies is called an acoustic harmonic series. If the source of these harmonics is a vessel propeller, the series is called a PSBHS.

Two types of discrete components can be distinguished in a PSBHS: the shaft and blade harmonic series. The first discrete component of the shaft harmonic series corresponds to the rotational frequency of the shaft, which is directly related to the vessel speed [2, 4]. The basic frequency of the blade

harmonic series is determined by the product of the shaft frequency and the number of propeller blades. Thus, by analyzing a PSBHS, it is possible to obtain valuable information about the vessel design, including the number of propeller blades, which is actively used in marine target recognition systems based on signal spectrum analysis [5].

Modern hydroacoustic systems analyze such signals with high accuracy. However, despite the well-developed algorithms of data processing, the final decision is mostly made by the operator [6]. The number of propeller blades is determined based on the spectrum parameters of the PSBHS presented to the operator.

Among the signal processing methods, note wavelet analysis, which allows detecting hydroacoustic signals in the form of a harmonic series and measuring the fundamental frequency of the shaft harmonic series [4]. Another approach is spectral analysis with the sequential extraction of particular discrete components and formation of the corresponding harmonic series [3].

For operator convenience, the results of narrowband frequency analysis are commonly presented in two forms: the spectrum graph, showing the location of signal harmonics, and the parameter table of detected discrete components and their characteristics. When analyzing the spectrum graph, the operator visually identifies the harmonics in order to distinguish among them the main shaft and blade frequencies. As a rule, the shaft frequency is the first discrete component, whereas the blade frequency is a subsequent one with maximum amplitude. In addition, the parameter table of the discrete components provides the operator with numerical values of the frequencies, increasing the accuracy of identification and reducing the probability of error.

Modern research aims at developing automated algorithms to decrease the dependence of analysis on the human factor. The conventional tool for analyzing acoustic noise is the *Fast Fourier Transform* (FFT), which extracts the main harmonic components of a signal. However, FFT has limited resolution, especially in low-signal and high-noise conditions. To overcome these limitations, the method of periodograms and autocorrelation analysis methods are used. For example, Welch's method reduces the scatter of power spectral density estimates [7]; MDVR (*Minimum Variance Distortionless Response*), MUSIC (*MUltiple SIgnal Classification*), and ESPRIT (*Estimation of Signal Parameters via Rotational Invariant Techniques*) provide superresolution [8].

Autocorrelation is effective in the analysis of weak signals and allows identifying regular patterns even under strong noise. Spectral envelope analysis is also actively used for extracting the characteristics of blade noise. An adaptive spectral envelope analysis technique introduced in [9] considers the effect of fluctuations in the spectrum.

In this paper, we propose several approaches to studying a mixture of a harmonic series and noise; when used together, they yield an estimate for the harmonic series base even under a small signal-to-noise ratio (SNR) for a single time window. The idea is to use the logarithm of the power spectrum of the signal under study. The envelope of the logarithm of the power spectrum is estimated by iterative averaging over three points. As shown below, this method is very close to the convolution of the spectrum and the Gaussian function, but three-point averaging allows estimating the harmonic series base with smaller errors. Next, the pseudospectrum (the difference between the logarithm of the power spectrum and its envelope) is analyzed.

The method of successive autocorrelations does not necessarily give a correct estimate for the harmonic series base. The result is influenced by the density of spectral lines, the value of the harmonic series base, and the noise level. To increase the sensitivity of this method, before applying autocorrelation, we "blur" the harmonic discrete samples a little by slightly smoothing the pseudospectrum.

After several successive autocorrelations, we calculate the so-called cepstral phase or saphe using the Hilbert transform (see the explanation in Section 1). The point is that after successive autocorrelations of the pseudospectrum, the result resembles a decreasing harmonic in the time domain, but the series itself relates to the frequency domain. Therefore, by applying the Hilbert transform to the autocorrelation of the pseudospectrum, we actually estimate the cepstral phase; when divided by the frequency to which this phase relates, the resulting value gives an estimate of the harmonic series base.

With the development of artificial intelligence methods, neural network models for classifying vessels based on their acoustic signals have become popular. *Convolutional Neural Networks* (CNNs) trained on noise spectrograms were considered in [10, 11]. Machine learning approaches improve the accuracy of determining propeller parameters but require large amounts of training data. Despite advances in automation, operator involvement remains

an important element of the analysis, especially in complex acoustic environments with possible interference and false responses.

DEMON (*Demodulation of Envelope Modulation On Noise*) is a special method for detecting modulations arising from the envelope of propeller cavitation. DEMON serves to extract the cavitation noise from the overall signal spectrum and determine the number of shafts, the rotational frequency of a shaft, and the number of propeller blades. In bioacoustics, this method is used to analyze the signals of whales, dolphins, and other animals. The limitation of this method is the need to select the noise band, which requires good skills of the hydroacoustic operator. Low interference immunity is another disadvantage of this method. The algorithm proposed below, utilizing three-point smoothing of the logarithm of the power spectrum, pseudospectrum pre-filtering, several successive autocorrelations, and the Hilbert transform, significantly improves interference immunity in PSBHS base estimation.

1. PROBLEM STATEMENT AND DETAILED DESCRIPTION OF FUNDAMENTAL FREQUENCY ESTIMATION STAGES

Now we formulate the main problem of this research. Let $\{x_k\}_{k=1}^{N}$ be a discrete series containing the sound recordings of sea vessel noise in a time window of size T (in seconds), with N samples in one window, $k \in [1, N]$, and $N = T f_s$, where f_s is the sampling frequency. It is required to develop an algorithm for estimating the PSBHS base f_0 by one time window and determine the optimal parameters of this algorithm.

The flowchart of the PSBHS base estimation algorithm is described in Fig. 1.

Periodogram construction

The periodogram is calculated using the *Discrete Fourier Transform* (DFT) for the signal x_k of length N:

$$X_j = \sum_{k=0}^{N-1} x_k e^{-i\frac{2\pi}{N}jk},$$

where X_j denotes the complex value of the spectrum at the jth frequency ($j = 0, 1, \ldots, N/2$), the frequency value in Hz is calculated as $f_j = j\dfrac{f_s}{N}$. Further, the algorithm deals only with a frequency range $f_{\min} \le f_j \le f_{\max}$. This limitation is due to, first, the absence of harmonic series components at frequencies above $f_{\max}$ and, second, the presence of strong noise at frequencies below $f_{\min}$. Hence, $N\dfrac{f_{\min}}{f_s} < j < N\dfrac{f_{\max}}{f_s}$.

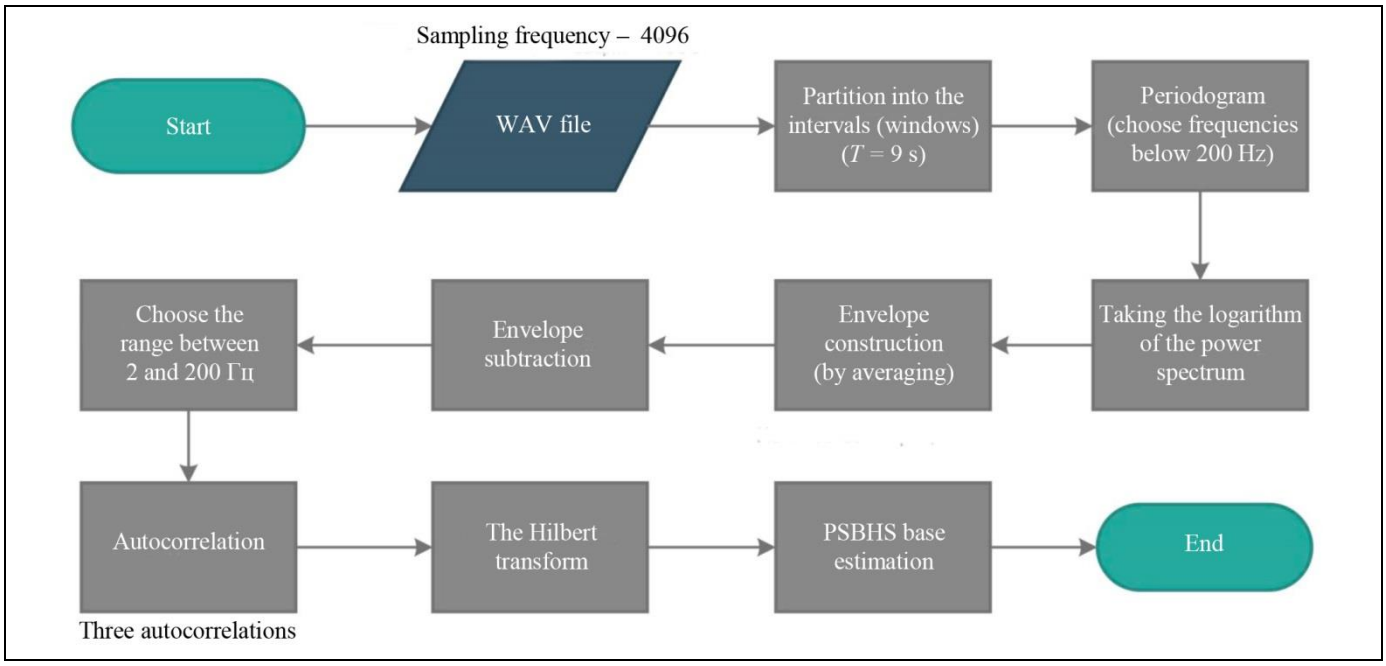

Fig. 1. The flowchart of the PSBHS base estimation algorithm.

Taking the logarithm of the periodogram

Taking the logarithm of the power spectrum of the signal eliminates sharp jumps associated with harmonics of the PSBHS, and the envelope can be separated by smoothing:

$$S_j^{(0)} = \ln |X_j|^2 .$$

Iterative spectrum smoothing

The spectrum envelope is constructed by averaging over three points in M iterations:

$$S_j^{(m)} = \frac{S_{j-1}^{(m-1)} + S_j^{(m-1)} + S_{j+1}^{(m-1)}}{3}, \qquad (1)$$

where j is the element number in the spectral series $\left(N\frac{f_{\min}}{f_s} < j < N\frac{f_{\max}}{f_s} \right)$; m is the iteration number $(m \in [1, M])$; M is the total number of iterations.

We clarify that the spectrum limits make some corrections to the expression (1):

$$S_j^{(m)} = \begin{cases} S_j^{(m-1)} \\ \quad \text{(for boundary points)} \\ \dfrac{S_{j-1}^{(m-1)} + S_j^{(m-1)} + S_{j+1}^{(m-1)}}{3} \\ \quad \text{(for inner points).} \end{cases} \qquad (2)$$

Definition 1. The iterative smoothing algorithm (2) of the series will be called the three-point smoothing of order M. ♦

The corrections in the final three-point smoothing algorithm (2) cover the effect of boundary points and insignificantly contribute to the spectrum smoothing results under $M \ll N$. Therefore, to simplify the proofs, the mathematical calculations below use the expression (1).

Note that M iterations in (1) are almost equivalent to weighting the original series elements by the Gaussian function with a standard deviation of $\sigma \approx \sqrt{\frac{2M}{3}} \approx 0.820467\sqrt{M}$. Examples for $M = 5$ and $M = 50$ are given in Fig. 2. (Also, see an example for M = 1,..., 4 in the table below.)

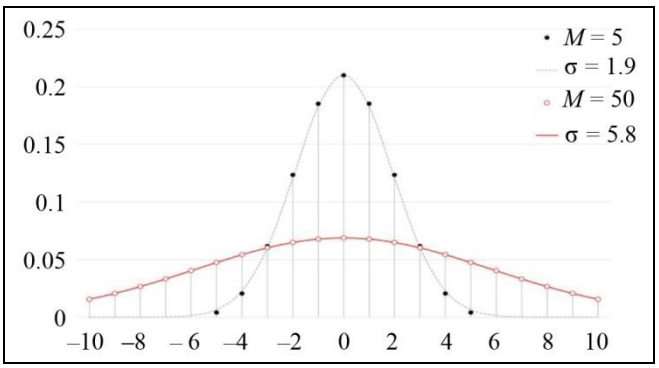

Fig. 2. The corresponding weights of the series elements obtained by formula (1) for M = 5 and M = 50 and the Gaussian function ($\sigma = \sqrt{2M/3}$): a visual comparison. The abscissa axis shows the deviations of the element number of the original series from j when estimating the weights.

Let us formulate the following result.

Lemma 1 (weight calculation). The M *successive iterations* (1) *generate the weights that can be approximately estimated using the Gaussian function with the parameter* $\sigma = \sqrt{\frac{2M}{3}}$ $(M >> 1)$:

$$S_j^{(M)} = \sum_{k=-M}^{M} \left[\frac{S_{j+k}^{(0)}}{\sqrt{4\pi M/3}} \exp\left(-\frac{k^2}{4M/3} \right) \right]. \qquad (3)$$

The weights of the three-point smoothing algorithm depending on the iteration number

m	$j-4$	$j-3$	$j-2$	$j-1$	j	$j+1$	$j+2$	$j+3$	$j+4$
1				$\frac{1}{3}$	$\frac{1}{3}$	$\frac{1}{3}$			
2			$\frac{1}{9}$	$\frac{2}{9}$	$\frac{3}{9}$	$\frac{2}{9}$	$\frac{1}{9}$		
3		$\frac{1}{27}$	$\frac{3}{27}$	$\frac{6}{27}$	$\frac{7}{27}$	$\frac{6}{27}$	$\frac{3}{27}$	$\frac{1}{27}$	
4	$\frac{1}{81}$	$\frac{4}{81}$	$\frac{10}{81}$	$\frac{16}{81}$	$\frac{19}{81}$	$\frac{16}{81}$	$\frac{10}{81}$	$\frac{4}{81}$	$\frac{1}{81}$
					...				

P r o o f. The fact that the weights obtained through successive iterations can be estimated by the Gaussian function is established technically. We show that in M iterations, the weights with the three-point averaging (1) are approximated by the Gaussian function with the parameter $\sigma = \sqrt{\frac{2M}{3}}$.

Let M be sufficiently large and consider iteration $M+1$; given that the weights in the three-point averaging algorithm at step M are approximated by the Gaussian function with the parameter $\sigma_M^2 = \alpha M$, for $j \ll M$ we have

$$\frac{1}{3\sigma\sqrt{2\pi}}\left(e^{-\frac{(j-1)^2}{2\sigma^2}} + e^{-\frac{(j)^2}{2\sigma^2}} + e^{-\frac{(j+1)^2}{2\sigma^2}}\right)$$

$$\approx \frac{1}{3\sigma\sqrt{2\pi}}\left(1-\frac{(j-1)^2}{2\sigma^2}+1-\frac{(j)^2}{2\sigma^2}+1-\frac{(j+1)^2}{2\sigma^2}\right)$$

$$= \frac{1}{\sigma\sqrt{2\pi}}\left(1-\frac{1}{2\sigma^2}\left(j^2+\frac{2}{3}\right)\right) \approx \frac{1}{\sigma\sqrt{2\pi}}\,\frac{1}{\left(1+\frac{1}{3\sigma^2}\right)}\,e^{-\frac{j^2}{2\sigma^2}}.$$

At step $M+1$, the coefficient at the exponent must be determined by the new parameter $\sigma_{M+1}^2 = \alpha(M+1)$. Therefore,

$$\sigma_{M+1}^2 = \alpha(M+1) = \alpha M + \alpha \approx \alpha M\left(1+\frac{1}{3\alpha M}\right)^2 \approx \alpha M + \frac{2}{3}.$$

It immediately follows that $\alpha = \frac{2}{3}$ and, accordingly, $\sigma = \sqrt{\frac{2M}{3}}$. ♦

We proceed to the next results.

Lemma 2 (spectrum smoothing by convolution). *The smoothing result with M successive iterations* (1) *applied to the logarithm of the power spectrum of the signal in a time window T can be approximately estimated by the convolution of this logarithm and the Gaussian function with the parameter* $\sigma = \frac{1}{T}\sqrt{\frac{2M}{3}}$ ($M >> 1$):

$$S_j^{(M)} = \sum_{k=-M}^{M}\left[S_{j+k}^{(0)}\sqrt{\frac{3}{\pi}}M^{-\frac{1}{2}}\exp\left(-\frac{3k^2T^2}{4M}\right)\right]. \quad (4)$$

The alternative form is

$$S^{(M)}(f) = S^{(0)}(f) * N(f,\sigma). \quad (5)$$

P r o o f. When increasing the time window size T, the density of the spectral lines grows whereas the standard deviation (the parameter of the Gaussian function used to estimate the weights, see formula (3) in Lemma 1) is reduced proportionally to T. Observing the normalization condition of the Gaussian function, we obtain the desired expression (4). ♦

Lemma 3 (spectrum smoothing by the cepstrum and Gaussian function). *The smoothing result with M successive iterations* (1) *applied to the logarithm of the power spectrum of the signal in a time window T can be approximately estimated by the Fourier transform of the product of its cepstrum, $K(\tau) = F^{-1}\left[S^{(0)}(f)\right]$, and the Gaussian function with the parameter* $\sigma^* = T\sqrt{\frac{3}{2M}}$ ($M >> 1$):

$$S^{(M)} = F\left[K(\tau)\cdot N(\tau,\sigma^*)\right].$$

P r o o f. Note that the expression (5) is the convolution of the logarithm of the signal power spectrum and the Gaussian function. By the well-known formula for the Fourier transform of the product of two functions ($F[f\cdot g] = F[f] * F[g]$), the above expression is nothing but the Fourier transform of the product of the inverse Fourier transform of the logarithm of the power spectrum (which is the cepstrum) and the inverse Fourier transform of the Gaussian function in the frequency domain with the parameter $\sigma = \frac{1}{T}\sqrt{\frac{2M}{3}}$ (which is also the Gaussian function in the time domain with the parameter $\sigma^* = T\sqrt{\frac{3}{2M}}$). Also, see an example in Fig. 3a. ♦

Lemma 4 (line spectrum extraction). *The line spectrum $\hat{S}(f) = S^{(0)}(f) - S^{(M)}(f)$ of the signal (defined as its pseudospectrum above) can be approximately estimated in the following ways:*

– via the convolution of the logarithm of its power spectrum with the difference between the delta function $\delta(f)$ and the Gaussian function:

$$\hat{S}(f) = S^{(0)}(f) * \left(\delta(f) - N(f,\sigma)\right),$$

where $\delta(f) \approx N(f,\sigma_\delta)$ and $\sigma_\delta \ll \sigma$, with σ_δ determining the accuracy of the line spectrum and σ the degree of smoothness of the spectrum envelope.

– via the Fourier transform of the product of the cepstrum of the original signal and the difference between the constant and the Gaussian function:

$$\hat{S}(f) = F\left[K(\tau)\cdot\left(\Psi - N(\tau,\sigma^*)\right)\right],$$

where the cepstrum is $K(\tau) = F^{-1}\left[S^{(0)}(f)\right]$ and $\Psi = F^{-1}\left[\delta(f)\right]$ ($\delta(f) \approx N(f,\sigma^\delta)$).

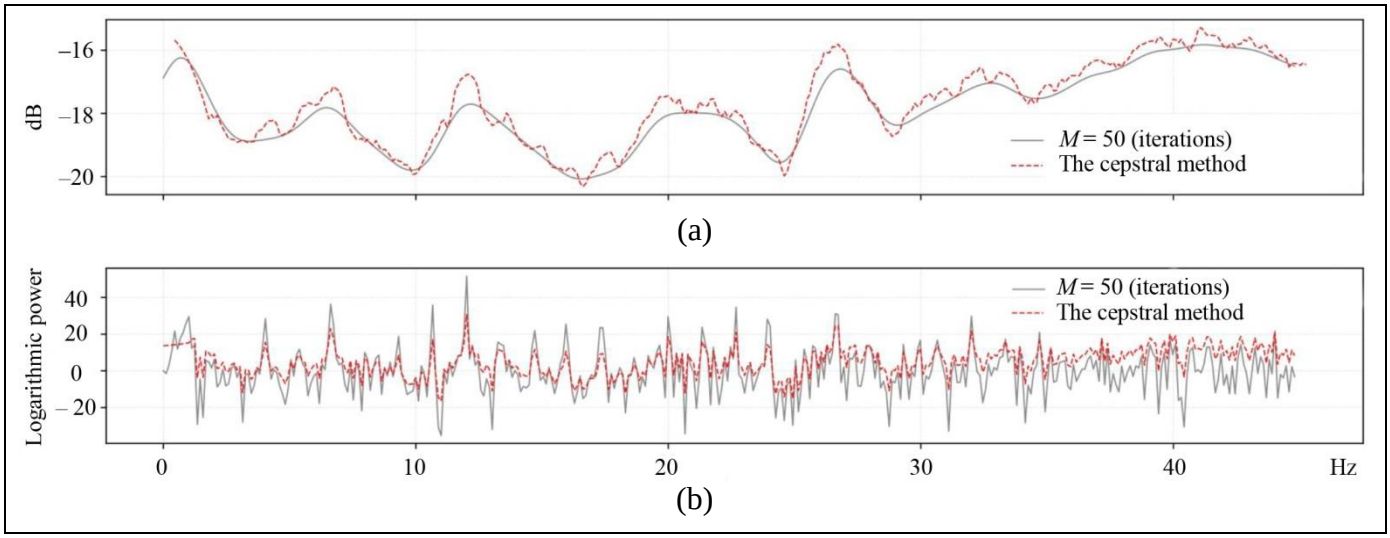

Fig. 3: (a) spectrum envelope estimation (Lemma 3) **and (b) centered logarithmic power spectrum** (Lemma 4). The estimates are obtained by two methods: iterative spectrum smoothing with envelope subtraction (solid lines) and envelope estimation with centered spectrum estimation via the cepstral method (dashed lines).

P r o o f. The desired result follows from Lemmas 2 and 3, the additivity of the Fourier transform, and the Fourier transform formula for the delta function:

$$\hat{S}(f) = S^{(0)}(f) - S^{(M)}(f) =$$

$$= S^{(0)}(f) - S^{(0)}(f) * N(f, \sigma)$$

$$= S^{(0)}(f) * (\delta(f) - N(f, \sigma)).$$

In turn, applying the Fourier transform formula for the product of two functions, we obtain

$$\hat{S}(f) = S^{(0)}(f) * (\delta(f) - N(f, \sigma))$$

$$= F\left[F^{-1}[S^{(0)}(f)] \cdot F^{-1}[(\delta(f) - N(f, \sigma))]\right]$$

$$= F\left[K(\tau) \cdot \left(\Psi - N(\tau, \sigma^*)\right)\right].$$

In numerical calculations with the discrete Fourier transform, an estimate of the delta function can be obtained from the Gaussian function with a small parameter $\sigma_\delta \ll \sigma$, with an appropriate normalization condition, the value $\Psi = F^{-1}\left[\delta(\tau)\right]$; see an example in Fig. 3b. (By the normalization condition, the sum of all weights obtained by the Gaussian function approximation must be 1.) ♦

Recall that cepstrum-related methods consider functions that can be viewed as spectra of logarithmic spectra. The concept of a cepstrum was introduced in 1963.

A power cepstrum is defined as "the power spectrum of a logarithmic power spectrum" [12]. Power cepstrum was proposed as a more efficient alternative to the autocorrelation function in detecting echoes in signals.

As the corresponding function describes the spectrum of a spectrum by definition, following a terminological analogy with "spectrum," A.S. Gol'din gave this function the name "cepstrum."[1]

However, the most important feature of cepstrum is not its representation as the spectrum of a spectrum but the associated logarithmic transformation of the original spectrum and the spectrum processed further. Note that the autocorrelation function, determined from the eigen power spectrum by the inverse Fourier transform, can also be treated as the "spectrum of a spectrum." In essence, the currently used notion of a cepstrum defines a power cepstrum as "the inverse Fourier transform of a logarithmic power spectrum." The difference between this definition and the definition of an autocorrelation function is only the logarithmic transformation of the original spectrum.

The application of power cepstra to study PSBHSs is based on the former's capability to detect spectrum periodicities, such as a series of uniformly distributed harmonics. From the standpoint of this application, an important advantage of cepstra is related to their small dependence on the propagation paths of signals, including the paths from sources to measurement points.

Trend subtraction and frequency range narrowing

Further, to separate the line spectrum, containing important information about a PSBHS, we subtract its envelope from the logarithm of the signal power

[1] Similarly, the terms "*quefrency*," "*rahmonic*," "*lifter*," "*gamnitude*," and "*saphe*" evolved from analogy with the conventional terms "*frequency*," "*harmonic*," "*filter*," "*magnitude*", and "*phase*." The terms related to "lifter" ("liftering," "liftered," etc.), indicating the filtering process in the cepstral domain, are occasionally used in the literature as well.

spectrum. In this case, the desired centered spectral series is given by

$$\hat{S}_j = \hat{S}(f_j) = S^{(0)}(f_j) - S^{(M)}(f_j) = S_j^{(0)} - S_j^{(M)}.$$

Then, an appropriate frequency range $f_j \in [f_{\min}, f_{\max}]$ is determined. Accordingly, the element number j of these frequencies satisfies the two-sided inequality $Tf_{\min} < j < Tf_{\max}$.

Successive autocorrelations

We apply several successive autocorrelations to the spectrum (precisely, to the centered logarithm of the spectral power) to smooth it further, improve pattern identification, and extract useful information from the spectrum more accurately.

Each autocorrelation calculation averages the information, removing noise components and short-term fluctuations. Performing several successive autocorrelations enhances this effect. Noise components often have a short period or random nature, and autocorrelation helps isolate regular and repeating elements. If the signal spectrum has a complex structure with several periodic components (contains several harmonic series), performing several autocorrelations will identify these components more accurately. With each autocorrelation step of the spectrum, more stable harmonic series are separated, whereas unstable ones and various noise are smoothed out. Therefore, several successive autocorrelations allow extracting the most stable component of propeller noise, i.e., the PSBHS base.

When analyzing the PSBHS, several successive autocorrelation steps for the logarithm of the power spectrum better isolate the low-frequency component (shaft frequency) against the background of the higher-frequency component (blade frequency). Note that when autocorrelation is applied to the spectrum, the low and high frequencies seem to change their places: the low-frequency shaft rotation is manifested by rapid peaks whereas the blade frequency by rarer peaks; after each autocorrelation, the shaft frequency is manifested more and more strongly.

The repeated autocorrelation of the spectrum is calculated for the smoothed result from its first autocorrelation, which gives additional smoothing. Since the noise components in the first autocorrelation are attenuated, averaging them again in the second autocorrelation even more damps both random bursts and non-harmonic components. However, there is a natural limitation: a very large number of autocorrelations will eventually smooth even useful information about stable, regular patterns that have long-term structure associated with the PSBHS base.

We define the autocorrelation function of the centered logarithmic power spectrum $\hat{S}_j$ of order $p = 0$ as follows:

$$C^{(0)}(f_k) = C_k^{(0)} = \sum_{j=Tf_{\min}}^{Tf_{\max}-k} \hat{S}_j \hat{S}_{j+k}.$$

Next, we define $C_k^{(p)}$ as the autocorrelation function of the centered logarithmic power spectrum $\hat{S}_j$ of order p:

$$C^{(p)}(f_k) = C_k^{(p)} = \sum_{j=Tf_{\min}}^{Tf_{\max}-k} C_j^{(p-1)} C_{j+k}^{(p-1)},$$

where $p \in [1, P]$ and $P + 1$ is the number of successive autocorrelations.

Hilbert transform

Modern methods of analytic signal theory [14] serve to extract (demodulate) an instantaneous amplitude (envelope), instantaneous phase, and instantaneous frequency from an oscillatory process. To obtain these instantaneous functions, one transforms an original process $x(t)$, defined on some interval, into the conjugate process $\hat{x}(t)$ using the *integral Hilbert transform* [5]:

$$\hat{x}(t) = \mathcal{H}\{x(t)\} = \frac{1}{\pi} \int_{-\infty}^{\infty} \frac{x(\tau)}{t - \tau} d\tau.$$

The analytic signal can be written as

$$x_a(t) = x(t) + i\hat{x}(t).$$

As is easily verified, the function $\sin \omega_0 t$ represents the Hilbert transform of the function $\cos \omega_0 t$. Therefore, the analytic signal corresponding to $\cos \omega_0 t$ is

$$x_a(t) = \cos \omega_0 t + i \sin \omega_0 t = \exp(i\omega_0 t).$$

It seems convenient to write a general analytic signal in exponential form as

$$x_a(t) = |x_a(t)| \exp\left[i\Phi(t)\right],$$

where

$$\begin{aligned} |x_a(t)| &= \left[x^2(t) + \hat{x}^2(t)\right]^{1/2}, \\ \Phi(t) &= \operatorname{arctg}\left[\hat{x}(t) / x(t)\right]. \end{aligned} \tag{6}$$

Now, by letting $\Phi(t) = \omega_0 t + \varphi(t)$, we have

$$x_a(t) = |x_a(t)| \exp\left[i\varphi(t)\right] \exp(i\omega_0 t) = \theta(t) \exp(i\omega_0 t).$$

The complex envelope $\theta(t)$ is obtained by removing the complex factor associated with the carrier from the analytic signal:

$$\theta(t) = x_a(t) \exp(-i\omega_0 t) = |x_a(t)| \exp\left[i\varphi(t)\right].$$

If $\theta(t)$ is a narrowband function relative to $\omega_0/2\pi$, it will have properties intuitively associated with the concept of envelope.

For an original signal in the frequency domain, the physical meaning of the integral Hilbert transform is the phase shift of all spectral components of this signal by $\pi/2$. The double Hilbert transform leads to the original process but with the opposite sign: it shifts the original signal by π.

We apply the Hilbert transform to $C^{(P)}(f_k)$ to obtain the *analytic autocorrelation*

$$\tilde{C}^{(P)}(f_k) = C^{(P)}(f_k) + i\mathcal{H}\{C^{(P)}(f_k)\}.$$

Here, the cepstral phase is defined as the argument of the analytic autocorrelation:

$$\varphi_k = \arg\tilde{C}^{(P)}(f_k) = \arg\left(C^{(P)}(f_k) + i\mathcal{H}\{C^{(P)}(f_k)\}\right),$$

$$\varphi_k = \operatorname{arctg}\left(\frac{\mathcal{H}\{C^{(P)}(f_k)\}}{C^{(P)}(f_k)}\right). \qquad (7)$$

Dwelling on these formulas, we introduce the following.

Definition 2. The *cepstral phase* is the value given by the expression (7). ♦

Let f_H denote the frequency for which the cepstral phase is calculated. Such a designation emphasizes that the saphe is calculated via the Hilbert transform.

Lemma 5 (the harmonic series base and the Hilbert transform). *Consider a given signal $x(t)$ with a non-constant amplitude and a frequency slowly changing during the entire observation period T. Then the average period $\overline{T_0}$ of signal oscillations over a time t can be estimated as*

$$\overline{T_0} = 2\pi t\left[\operatorname{arctg}\left(\frac{\mathcal{H}\{x(t)\}}{x(t)}\right)\right]^{-1},\ 0 < t < T.$$

The proof is technical and can be easily derived from the expression (6).

This lemma leads to the following result. Let the signal $x(t)$ in Lemma 5 be the correlogram $C^{(P)}$ of the logarithmic power spectrum of a signal-noise mixture containing a signal (a harmonic series with a base f_0) and some noise with a sufficiently high SNR value. Then the harmonic series base can be estimated as

$$f_0 = 2\pi f_H\left[\operatorname{arctg}\left(\frac{\mathcal{H}\{C^{(P)}(f_H)\}}{C^{(P)}(f_H)}\right)\right]^{-1}, \qquad (8)$$

where $f_{\min} < f_H < f_{\max}$.

Note that the frequency f_H should be assigned depending on a particular task and conditions. For example, under strong noise, the recommendation is to choose this frequency in the range $0.1f_{\max} < f_H < 0.2f_{\max}$ (the correlogram "breaks" at the right end due to the large noise component). On the other hand, $f_H \approx f_{\max}$ is recommended when estimating the PSBHS base with high accuracy in weak noise conditions. As is easily shown, the PSBHS base estimate (8) represents the averaging of the frequency differences of the autocorrelation peaks; in turn, this determines the estimation accuracy $T^{-1}\frac{f_0}{f_H}$, constituting thousandths of a hertz in practice. (For example, for a time window of $T = 10$ s, the PSBHS base is $f_0 \approx 1$ Hz, and the search range of the harmonic series modes is limited by the frequency $f_{\max} = 100$ Hz.)

In general, we underline that the harmonic series base estimation method (8) gives less error with increasing SNR, and relevant estimates can be obtained only above a certain threshold ($\mathrm{SNR} > \mathrm{SNR}_0$). Below, we demonstrate how this threshold can be reduced.

Figure 4 presents the results of a numerical experiment: $\Omega = (1 + \exp(-0.4364\cdot\mathrm{SNR} - 0.8545))^{-1}$ (the solid line, without smoothing) and $\Omega = (1 + \exp(-0.4212\cdot\mathrm{SNR} - 2.3633))^{-1}$ (the dashed line). Each point was constructed from 500 cases. Each case was obtained by generating a time series of length $N = 4096$ via summing a signal (a harmonic series) and white noise with the following parameters: $T = 1$s (time window), $d = 15$ (the number of harmonic series samples, with the same power level), $f_0 = 60$ Hz (the frequency difference between samples), and SNR = –12 dB,…, 7 dB.

As discovered, the pre-smoothing of the pseudospectrum allows reducing the SNR thresholds from 0 to –5 dB. In Fig. 4a, the optimum is achieved by 40 iterations of the three-point smoothing of the pseudospectrum; for this experiment, it is equivalent to the convolution of the pseudospectrum and the Gaussian function ($\sigma \approx 5$ Hz). Figure 4b shows a comparative analysis of the error-free harmonic series base estimates without smoothing (the lower curve) and with smoothing in 40 iterations (the upper curve). As a rule, the pseudospectrum in real sound recordings is more or less "blurred," and additional smoothing is not always necessary.

Next, Fig. 5 provides the histograms of the harmonic series base estimates for different SNR values of the harmonic series and white noise. One

thousand (1000) signal-noise mixtures were generated to construct each histogram. The frequency difference between harmonics was set equal to 60 Hz. No pre-smoothing of the pseudospectrum was performed.

Figure 6 shows the histograms of the harmonic series base estimates for SNR = –3 dB. Five thousand (5000) signal-noise mixtures were generated to construct each histogram. The frequency difference

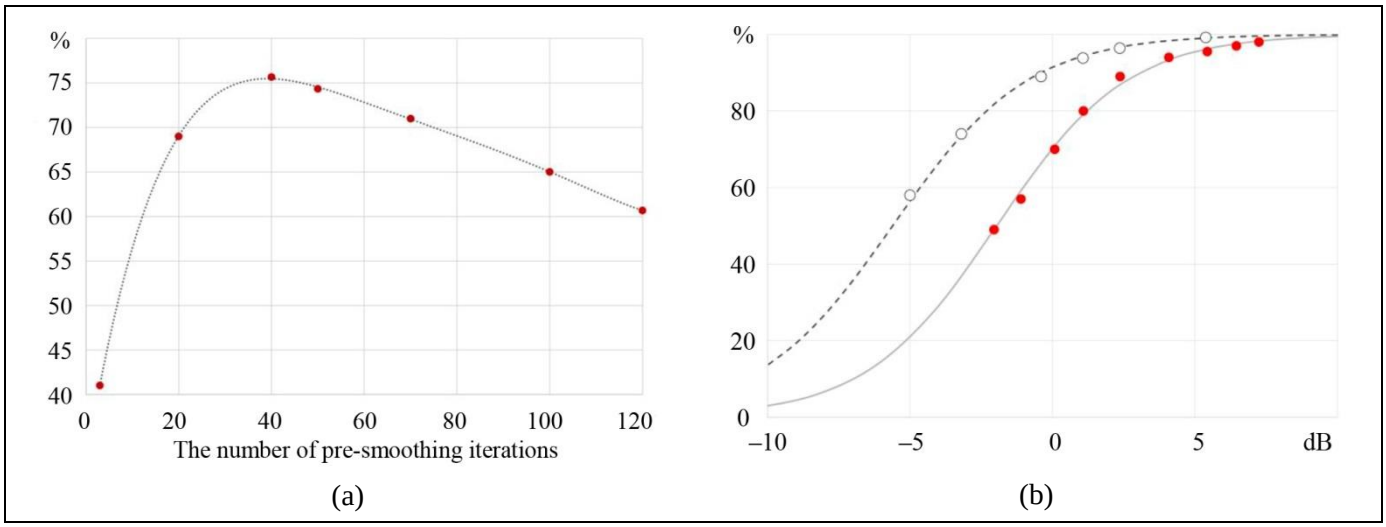

Fig. 4: (a) the share of error-free PSBHS base estimates Ω (SNR= –3 dB) depending on the pre-smoothing of the harmonic pseudospectrum and (b) a visual comparison of the dependences of error-free PSBHS base estimates without spectrum smoothing and with spectrum smoothing in 40 iterations.

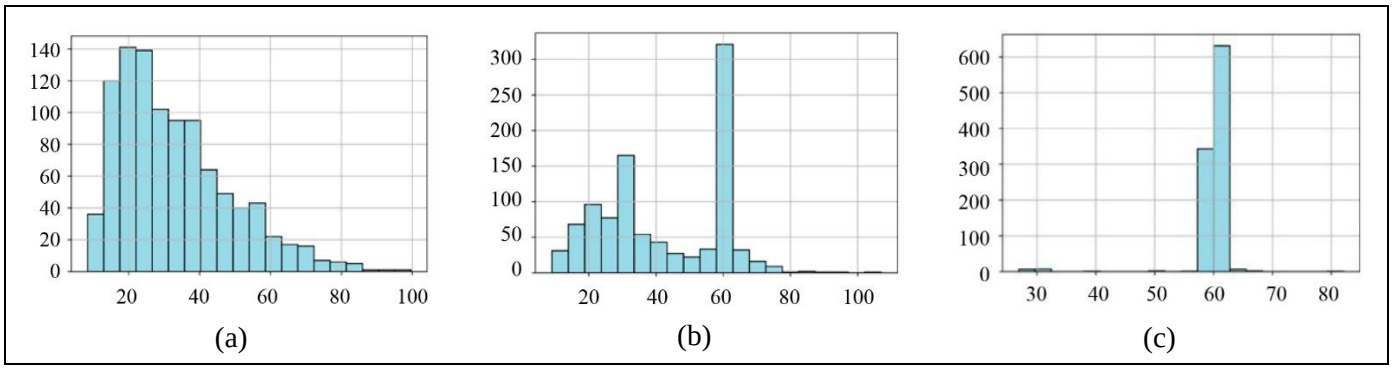

Fig. 5. The histograms of PSBHS bases for different SNR values (without smoothing): (a) SNR = – 12 dB, Ω = 1%, (b) SNR = – 3 dB, Ω = 40%, and (c) SNR = + 7 dB, Ω = 98%.

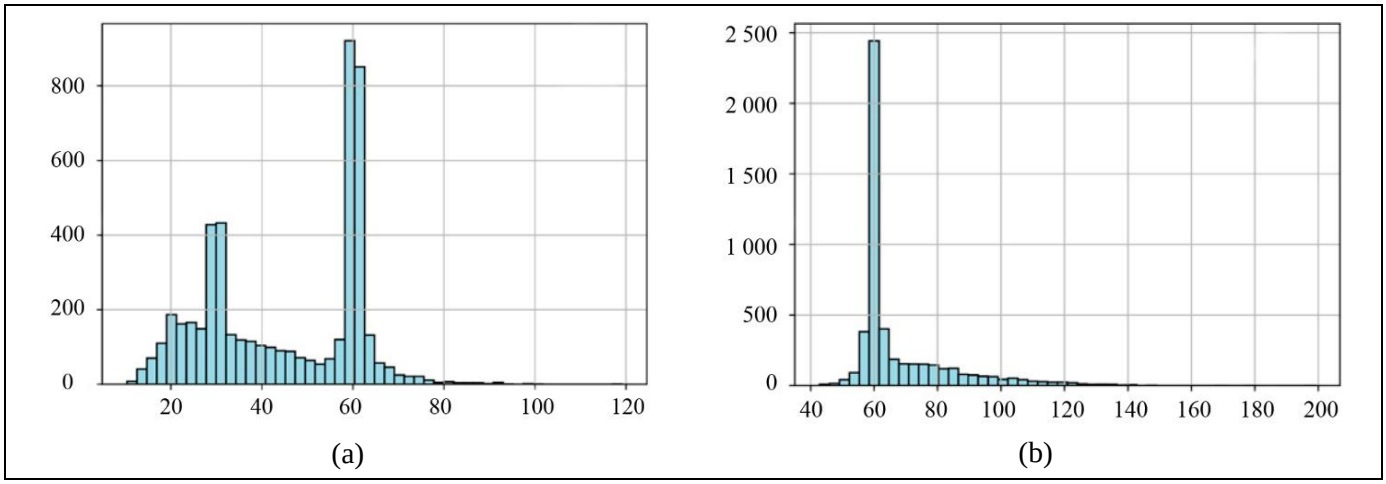

Fig. 6. The histograms of PSBHS bases for different smoothing methods, SNR = – 3 dB: (a) without smoothing, Ω = 40% and (b) with smoothing in 100 iterations, Ω = 65%.

between harmonics was set equal to 60 Hz. Figure 6a corresponds to the solution without smoothing; Fig. 6b, to the solution with the pre-smoothing (100 iterations over three points) of the spectrum of the signal-noise mixture.

2. THE PSBHS BASE ESTIMATION ALGORITHM: A BRIEF DESCRIPTION OF KEY STEPS

The PSBHS base estimation algorithm was tested on the real sound recordings of sea vessel noise, and the effectiveness of the iterative three-point smoothing method was validated for constructing the spectrum envelope. Also, the effectiveness of the PSBHS base estimation method with the convolution of the logarithm of the signal power spectrum and the difference of two Gaussian functions was validated.

Summarizing the outcomes, we write the main steps of the PSBHS base estimation algorithm using convolution:

1. Estimating the periodogram of the signal x_k of length N in a time window of size T:

$$X_j = \sum_{k=0}^{N-1} x_k e^{-i\frac{2\pi}{N}jk}.$$

2. Taking the logarithm of the power spectrum of this signal:

$$S_j^{(0)} = \ln |X_j|^2.$$

3. Extracting the line (centered) spectrum of the signal by convolution (M_0 blurring iterations for the centered spectrum and M spectrum smoothing iterations for envelope estimation, where $M_0 \ll M$ and $Tf_{\min} < j < Tf_{\max}$):

$$\hat{S}_k = S_j^{(0)} * \left[\frac{1}{\sqrt{M_0}} \exp\left(-\frac{j^2T^2}{M_0} \right) - \frac{1}{\sqrt{M}} \exp\left(-\frac{j^2T^2}{M} \right) \right].$$

Due to boundary effects, the mean value of the series $\hat{S}_k$ slightly differs from zero, and the mean value is subtracted from the obtained series before constructing the autocorrelation function.

4. Estimating the autocorrelation function of the centered spectrum:

$$C_k^{(0)} = \sum_{j=Tf_{\min}}^{Tf_{\max}-k} \hat{S}_j \hat{S}_{j+k},$$

$$C_k^{(p)} = \sum_{j=Tf_{\min}}^{Tf_{\max}-k} C_j^{(p-1)} C_{j+k}^{(p-1)},$$

where $p \in [1, P]$ and $P + 1$ is the number of successive autocorrelations.

5. Estimating the PSBHS base:

$$f_0 = 2\pi f_H \left[\operatorname{arctg}\left(\frac{\mathcal{H}\{C^{(P)}(f_H)\}}{C^{(P)}(f_H)} \right) \right]^{-1},$$

where $f_{\min} < f_H < f_{\max}$.

3. OPTIMAL PARAMETERS OF THE PSBHS BASE ESTIMATION ALGORITHM

Consider a set of PSBHS bases obtained by processing the sound recordings of sea vessel noises using the above algorithm:

$$F_0^{(r)} = \{ f_0^{(r)} \}_{i=1}^{Z_r},$$

where r is the WAV file number; $F_0^{(r)}$ is the set of PSBHS base estimates in each time window for the rth WAV file; Z_r is the total number of time windows in the rth WAV file; finally, Z_rT is the size of the sea vessel sound recording.

Among all WAV files, we take those satisfying the inequality $\sigma^{(r)} < \alpha T^{-1}$ ($\alpha \approx 10$), where $\sigma^{(r)}$ is the standard deviation of the PSBHS base estimates for the rth recording (i.e., the ones with an insignificant change of the PSBHS base estimates during the observation time). Erroneous estimates are such that

$$| f_0^{(r)} - \mu^{(r)} | > \alpha T^{-1},$$

where $\mu^{(r)}$ denotes the mean value of the PSBHS bases for the rth Wav file.

An optimal tuple of the parameters (T, M, $f_{\min}$, $f_{\max}$, P, and f_H) of the PSBHS base estimation algorithm is selected according to the criterion

$$\sum_r \omega^{(r)} \underset{T, M, f_{\min}, f_{\max}, P, f_H}{\rightarrow} \min,$$

where $\omega^{(r)}$ is the number of errors for the rth WAV file.

The following optimal parameters of the algorithm were obtained on real data on cargo and passenger sea vessels in terms of this criterion:

- T = 10 s (the time window size),
- $M = 100$ (the number of smoothing iterations given $M_0 = 10$ pre-smoothing iterations to blur the pseudospectrum),
- ($f_{\min} = 2$, $f_{\max} = 200$) Hz (the autocorrelation interval),

• $P = 2$ ($P + 1 = 3$ is the number of successive autocorrelations),

• $f_H = 25$ Hz (the frequency for estimating the "cepstral phase").

CONCLUSIONS

This paper has presented new approaches to estimating the fundamental frequency of a harmonic series from a single time window in high noise conditions. The algorithm for determining the base of a propeller shaft–blade harmonic series has demonstrated stable performance under a signal-to-noise ratio exceeding –5 dB. As expected, in future works, the method will be improved to get a refined base estimate by continuous signal processing over multiple time windows as well as by using information characteristics [15]. As shown above, an effective solution can be obtained via a set of measures and correctly chosen values of the algorithm parameters.

In the course of this study, numerical experiments have been conducted on the sound recordings of sea vessel noises (in total, over 400 sound recordings of passenger ships, container ships, tankers, and tugs). According to the experiment results, the methods are effective.

In several cases, when the sea vessel noise is generated by several propellers, beats have been observed. Consequently, it is difficult to determine the shaft frequency from separate time windows (in these windows, the signals at the shaft frequencies arrive in counter-phase). Here, one faces the validity problem of PSBHS base estimation, which is also the objective of subsequent research.

Also, this work is part of a group of approaches to investigating the noise spectra of sea vessels. Note that the identification and utilization of additional information criteria in other spectrum ranges of sea vessel noises significantly improves the estimation quality of the PSBHS base as well.

Acknowledgments. *This work was supported by the Russian Science Foundation, project no. 23-19-00134.*

REFERENCES

1. Urick, R.J., *Principles of Underwater Sound*, McGraw-Hill, 1975.
2. Evtyutov, A.P. and Mit'ko, V.B., *Primery inzhenernykh raschetov v gidroakustike* (Examples of Engineering Calculations in Hydroacoustics), Leningrad: Sudostroenie, 1981. (In Russian.)
3. Kudryavtsev, A.A., Luginets, K.P., and Mashoshin, A.I., Amplitude Modulation of Underwater Noise Produced by Seagoing Vessels, *Acoustical Physics*, 2003, vol. 49, no. 2, pp. 184–188.
4. Malyi, V.V., Saprykin, V.A., Rokhmaniiko, A.Yu., et al., Patent RU 2464588 C1, *Byull. Izobr*., 2012, no. 29.
5. Burdik, V.S., *Analiz gidroakusticheskikh sistem* (Analysis of Hydroacoustical Systems), Leningrad: Sudostroenie, 1988. (In Russian.)
6. Evtyutov, A.P., Kolesnikov, A.E., Korepin, E.A., et al., *Spravochnik po gidroakustike* (Hydroacoustics Handbook), Leningrad: Sudostroenie, 1988. (In Russian.)
7. Astfalck, L.C., Sykulski, A.M., and Cripps, E.J., Debiasing Welch's Method for Spectral Density Estimation, *arXiv:2312.13643*, 2023, pp. 1–17. DOI: https://doi.org/10.48550/arXiv.2312.13643
8. Knichuta, E.V., Pachotin, V.A., Budnik, S.S., and Rzhanov, A.A., The Signal Parameter Estimation Task Solution in the Frequency Domain for the Pulse Signals, *Journal of the Russian Universities. Radioelectronics*, 2005, no. 2, pp. 19–29. (In Russian.)
9. Marapulets, Yu.V., Adaptive Spectral Analysis of the Amplitude Envelope of Marine Vessel Noise, *Bulletin of the Kamchatka State Technical University*, 2003, no. 2, pp. 52–60. (In Russian.)
10. Liu, D., Yang, H., Hou, W., and Wang, B., A Novel Underwater Acoustic Target Recognition Method Based on MFCC and RACNN, *Sensors*, 2024, vol. 24, no. 1, art. no. 273.
11. Doan, V.-S., Huynh-The, T., and Kim, D.-S., Underwater Acoustic Target Classification Based on Dense Convolutional Neural Network, *IEEE Geoscience and Remote Sensing Letters*, 2022, vol. 19, art no. 15009052020, pp. 1–5. DOI: 10.1109/LGRS.2020.3029584
12. Randall, R.B., *Frequency Analysis*, Naerum: Brüel & Kjaer, 1987.
13. Gol'din, A.S., *Vibratsiya rotornykh mashin* (Vibration of Rotary Machines), Moscow: Mashinostroenie, 2000. (In Russian.)
14. Genkin, M.D. and Sokolova, A.G., *Vibroakusticheskaya diagnostika mashin i mekhanizmov* (Vibroacoustical Diagnosis of Machines and Mechanisms), Moscow: Mashinostroenie, 1987. (In Russian.)
15. Galyaev, A.A., Babikov, V.G., Lysenko, P.V., and Berlin, L.M., A New Spectral Measure of Complexity and Its Capabilities for Detecting Signals in Noise, *Doklady Mathematics*, 2024, vol. 110, pp. 361–368.

This paper was recommended for publication by B. V. Pavlov, a member of the Editorial Board.

Received April 15, 2025, and revised June 5, 2025.
Accepted June 25, 2025

Author information

Babikov, Oleg Vladimirovich. Mathematician, Trapeznikov Institute of Control Sciences, Russian Academy of Science, Moscow, Russia
✉ babikov.ov@phystech.edu

Babikov, Vladimir Georgievich. Cand. Sci. (Phys.–Math.), Trapeznikov Institute of Control Sciences, Russian Academy of Sciences, Moscow, Russia
✉ babikov@ipu.ru

Cite this paper

Babikov, O.V., and Babikov, V.G., Estimating the Fundamental Frequency of a Propeller Shaft–Blade Harmonic Series Using the Hilbert Transform and Autocorrelation. *Control Sciences* **3,** 12–23 (2025).

Original Russian Text © Babikov, O.V., Babikov, V.G., 2025, published in *Problemy Upravleniya*, 2025, no. 3, pp. 58–73.

Translated into English by *Alexander Yu. Mazurov*,
Cand. Sci. (Phys.–Math.),
Trapeznikov Institute of Control Sciences, Russian Academy of Sciences, Moscow, Russia
✉ alexander.mazurov08@gmail.com